BIOLOGY OF REPRODUCTION (2012) **86**(5):155, 1–10
Published online before print 18 January 2012.
DOI 10.1095/biolreprod.111.095430

The Spermatogonial Stem Cell Niche in the Collared Peccary (*Tayassu tajacu*)[1]

Paulo Henrique A. Campos-Junior,[3] Guilherme M.J. Costa,[3] Samyra M.S.N. Lacerda,[3] José V. Rezende-Neto,[3] Ana M. de Paula,[4] Marie-Claude Hofmann,[5] and Luiz R. de França[2,3]

[3]*Laboratory of Cellular Biology, Department of Morphology, Federal University of Minas Gerais, Belo Horizonte, Minas Gerais, Brazil*
[4]*Biophotonics Laboratory, Department of Physics, Federal University of Minas Gerais, Belo Horizonte, Minas Gerais, Brazil*
[5]*Department of Comparative Biosciences, University of Illinois, Urbana-Champaign, Illinois*

ABSTRACT

In the seminiferous epithelium, spermatogonial stem cells (SSCs) are located in a particular environment called the "niche" that is controlled by the basement membrane, key testis somatic cells, and factors originating from the vascular network. However, the role of Leydig cells (LCs) as a niche component is not yet clearly elucidated. Recent studies showed that peccaries (*Tayassu tajacu*) present a peculiar LC cytoarchitecture in which these cells are located around the seminiferous tubule lobes, making the peccary a unique model for investigating the SSC niche. This peculiarity allowed us to subdivide the seminiferous tubule cross-sections in three different testis parenchyma regions (tubule-tubule, tubule-interstitium, and tubule-LC contact). Our aims were to characterize the different spermatogonial cell types and to determine the location and/or distribution of the SSCs along the seminiferous tubules. Compared to differentiating spermatogonia, undifferentiated spermatogonia (A_{und}) presented a noticeably higher nuclear volume ($P < 0.05$), allowing an accurate evaluation of their distribution. Immunostaining analysis demonstrated that approximately 93% of A_{und} were GDNF receptor alpha 1 positive ($GFRA1^+$), and these cells were preferentially located adjacent to the interstitial compartment without LCs ($P < 0.05$). The expression of colony-stimulating factor 1 was observed in LCs and peritubular myoid cells (PMCs), whereas its receptor was present in LCs and in $GFRA1^+$ A_{und}. Taken together, our findings strongly suggest that LCs, different from PMCs, might play a minor role in the SSC niche and physiology and that these steroidogenic cells are probably involved in the differentiation of A_{und} toward type A_1 spermatogonia.

CSF1R, GDNF, GFRA1, Leydig cells, Sertoli cells, spermatogenesis, spermatogonial stem cell niche, spermatogonial stem cells (SSCs), testis

INTRODUCTION

Spermatogonial stem cells (SSCs) form the tissue-specific stem cell population of spermatogenesis and are committed to the establishment and maintenance of spermatogenesis [1]. SSCs provide this function by undergoing both self-renewal and differentiation [1]. Self-renewal continually provides a pool of SSCs (often referred to as A_{single} [A_s] spermatogonia), whereas differentiation results in formation of A_{paired} (A_{pr}) spermatogonia followed by $A_{aligned}$ (A_{al}) spermatogonia, forming chains of 4, 8, 16, and 32 cells (A_{al4}, A_{al8}, A_{al16}, and A_{al32}, respectively) [2–4]. A_{al} spermatogonia differentiate into type A_1 spermatogonia that produce types A_2 to A_4 spermatogonia, which give rise to intermediate (In) and type B spermatogonia [1]. Recent studies demonstrated that some undifferentiated (A_{und}) spermatogonia (A_s to A_{al8}) maintain stemness potential [5]. They are able to differentiate into more mature germ cells but can revert into new A_s spermatogonia by spermatogonial clone fragmentation in certain conditions [5]. The spermatogonial subtypes and kinetics described so far are typical for rodents and, therefore, may be different in other species [1–5]. Besides transmitting genetic information to the next generation, SSCs represent a unique type of stem cells, because they are also able to convert into pluripotent cells that can differentiate into somatic tissues [6]. Therefore, investigating SSC physiology is a crucial aspect of reproductive biology. Indeed, such study will lead to a better understanding of some causes of male infertility and to the development of novel cellular models for tissue engineering [6, 7].

In the testis, SSCs reside within a specific microenvironment called the ''niche,'' which regulates self-renewal, quiescence, and commitment to differentiation [8–13]. However, others have suggested that this microenvironment will preferentially regulate self-renewal, whereas differentiation will take place outside the niche [14]. Studies performed in mice [8], rats [9], hamsters [10], and donkeys [11] have shown that SSCs are preferentially located in the region adjacent to the interstitial compartment of the testis. This particular location is considered as the niche, which may be controlled by the Sertoli and peritubular myoid cells, basement membrane, and other cellular components/factors from the intertubular compartment [7–9, 12, 13]. In mice, Yoshida et al. [15] reported that the vascular network likely plays an important role in the distribution and fate of A_{und} spermatogonia.

Glial cell-derived neurotrophic factor (GDNF), produced by Sertoli cells under the influence of follicle-stimulating hormone, is the most important niche factor for SSC self-renewal and maintenance [12]. GDNF signals through a membrane receptor complex formed by the GDNF receptor α1 (GFRA1) and the receptor tyrosine kinase RET (REarranged during Transfection), both expressed by SSCs [12, 16, 17]. In addition, Leydig and peritubular myoid cells might participate in the regulation of the niche [12, 13], because both cell types produce colony-stimulating factor 1 (CSF1), whereas SSCs express the CSF1 membrane receptor (CSF1R) [17, 18]. The existence of a small population of GFRA1-positive ($GFRA1^+$) [17] and Thy-1-positive ($Thy\text{-}1^+$) [18] spermatogonia that also expressed the CSF1R ($CSF1R^+$) was shown. When these double-positive SSCs ($Thy\text{-}1^+/CSF1R^+$ or $GFRA1^+/CSF1R^+$) were cultured in vitro in the presence of CSF1, they proliferated and showed an increased self-renewing

[1]Supported by FAPEMIG, CNPq, and NIH-HD044543 (M.C.H.).
[2]Correspondence: E-mail: lrfranca@icb.ufmg.br

Received: 6 August 2011.
First decision: 1 September 2011.
Accepted: 27 December 2011.

eISSN: 1529-7268 http://www.biolreprod.org
ISSN: 0006-3363

ability [17, 18]. Although Leydig cells may be involved in the regulation of the testicular SSC niche in mammals, their exact role remains unclear, probably because they are uniformly distributed in the interstitial compartment in all species so far investigated [7–9, 11, 15].

Recent studies performed in our laboratory showed that the collared peccary (*Tayassu tajacu* Linnaeus, 1758), a suiform species, presents a unique Leydig cell organization and distribution around the seminiferous tubule lobes [19], which are classically defined as a portion of the testis parenchyma containing convoluted seminiferous tubules externally delimited by connective tissue [20, 21]. Because of this particular cytoarchitecture, collared peccaries may represent a suitable and unique experimental model for investigating SSC physiology and niche. Thus, the present study was developed to further characterize the collared peccary testis parenchyma. We were particularly interested in investigating the morphology, phenotype, and kinetics of spermatogonia and in evaluating the location/distribution of SSCs. To better understand the role of Leydig cells in the SSC niche, we also investigated several soluble factors that may be involved in SSC physiology.

MATERIALS AND METHODS

Animals and Tissue Preparation

Eighteen adult collared peccaries were used in the present study. The animals were obtained from Engenho d'Água commercial farm (Ouro Preto, MG, Brazil) located in the southeastern region of Brazil. Testes sampling was performed by orchiectomy, and all surgical procedures were performed by a veterinarian following approved guidelines for the ethical treatment of animals. The testes were separated from the epididymis and weighed, then cut longitudinally with a razor blade into small fragments. Testes from eight animals were fixed by immersion in 4% buffered glutaraldehyde for 12 h. Tissue samples (thickness, 2–3 mm) were routinely processed and embedded in plastic glycol methacrylate (Leica HistoResin) for histological and stereological analyses. To characterize the different spermatogonial types using high-resolution microscopy, the samples (thickness, 1–2 mm) were prepared as described by Chiarini-Garcia and Russel [22]. As described in other sections, testes samples from 10 other animals were used for Western blot analysis (n = 4) and immunostaining (n = 6).

Stages of the Seminiferous Epithelial Cycle and Stereological Analyses

The stages of the seminiferous epithelial cycle of collared peccaries were characterized based on the development of the acrosomal system of the spermatids and in the overall germ cell associations [23, 24]. The relative stage frequencies were determined from 150 seminiferous tubule cross-sections per animal.

The volume density of Leydig cells and blood vessels in the testis parenchyma were determined by light microscopy using a 441-intersection grid placed in the ocular of the microscope. Approximately 15 500 points per animal were counted in the testis parenchyma that also encompassed the two evaluated spaces (Leydig cell cord and intertubular space). The obtained data related to the Leydig cells and blood vessels were initially expressed as a percentage occupied by these two components. Subsequently, considering the testis parenchyma volume [19], Leydig cell and blood vessel volume density in two evaluated spaces were expressed in microliters. Artifacts were rarely seen and were not considered in the total number of points used to obtain the volume densities.

The nuclear volume of Leydig cells was obtained from the knowledge of the mean nuclear diameter, and 60 nuclei were measured for each animal. Leydig cell nuclear volume was expressed in cubic micrometers and obtained by using the formula $4/3\pi r^3$, where r = nuclear diameter/2.

Spermatogonial Morphology, Size, Kinetics, and Distribution

The morphological characterization of the different spermatogonial types was performed through the analysis of images obtained from the spermatogonial cells present in each stage of the seminiferous epithelial cycle [22]. For this purpose, the following morphological nuclear features were evaluated: shape of the nucleus, presence and disposition of heterochromatin, granularity of the euchromatin, and extent of the nucleolus compaction. The spermatogonial cells were grouped by each stage of the seminiferous epithelial cycle according to their morphological characteristics. The nuclear diameter of each spermatogonial type was obtained by the measurement of 30 nuclei of each cell type per animal. The spermatogonial kinetics was performed by counting the different spermatogonial cells present in each stage of the seminiferous epithelial cycle, and their number was expressed as a ratio per 1000 Sertoli cell nuclei [11].

To evaluate the distribution of the spermatogonial cells, images from 10 seminiferous tubule cross-sections of each stage of the seminiferous epithelial cycle previously characterized were obtained for each animal. The seminiferous tubule cross-sections were subdivided into three regions characterized as follows: adjacent to another tubule (tubule-tubule [T-T]), adjacent to the interstitial compartment without Leydig cells (tubule-interstitium [T-I]), and adjacent to the interstitial compartment containing Leydig cells (tubule-Leydig cells [T-LC]). Considering that the tubular circumference has 360°, the numbers of spermatogonia (A_{und}, A_1, A_2, A_3, A_4, In, and B) obtained in the three different regions evaluated were expressed per degree. Therefore, it allowed an estimation of the spermatogonial cell population and location in each region. Also, to provide a more precise evaluation regarding the spermatogonial cell preferential location and to verify the existence of an eventual distribution gradient, the three regions described were subdivided in peripheral and central areas. The same kind of analysis was performed in the inner seminiferous tubules that do not face the Leydig cell cords. Therefore, in this analysis, only T-T and T-I regions were evaluated.

In addition, to evaluate the eventual influence of the vascular network in the spermatogonial distribution, the number of A_{und} and differentiated spermatogonia, as well as the number of Sertoli cell nuclei, were counted in the T-I region with or without blood vessels, according to noticeable or conspicuous blood vessel criteria.

Western Blot Analysis

To qualitatively evaluate the presence of specific markers for SSCs (GFRA1 and CSF1R) and factors (CSF1) related to spermatogonial self-renewal already identified in other mammalian species, Western blot analysis was performed using total protein lysates from collared peccary testes. For this evaluation, 300 mg of testis parenchyma from four adult animals were placed in 0.9% NaCl containing protease inhibitors (Sigma-Aldrich), and the tissues were homogenized and sonicated. After sonication, the lysates were centrifuged at 14 000 × *g* for 30 min. Supernatants were collected and then frozen at −80°C. Protein samples were diluted 1:2 in a solution of 10% SDS (Sigma-Aldrich), glycerol, and 10% bromophenol blue in 0.5 M Tris buffer (pH 6.8), and the samples were boiled for 5 min.

Denatured 12% SDS-polyacrylamide minigels were prepared, and 20-μl samples were loaded into the wells. High-molecular-weight markers (Sigma-Aldrich) were run parallel to the samples. Gels were run with a 90-mA current and separated proteins transferred onto a nitrocellulose filter for 75 min by using a 100-mA current. The strips were blocked with 1% bovine serum albumin (Sigma-Aldrich) in PBS for 1 h at room temperature. Then, the strips were incubated for 120 min at room temperature with anti-GFRA1 antibody (SC-6157, 1:500; Santa Cruz Biotechnology), anti-CSF1 antibody (Ab1324, 1:200; Abcam), and anti-CSF1R antibody (Ab61137, 1:200; Abcam). After incubation, the strips were washed three times with Tris-buffered saline (TBS)-0.05% Tween solution and then incubated for 1 h in biotinylated anti-goat or anti-rabbit immunoglobulin (IgG) antibodies (Ab6740 and Ab6720; 1:100 and 1:200, respectively; Abcam). The strips were washed three times with TBS-0.05% Tween solution, 5 min each, and incubated in streptavidin solution (TS-125-HR; Thermo Scientific) for 15 min, at room temperature. These strips were then washed three times with TBS-0.05% Tween solution, 5 min each, and incubated with 3,3′-diaminobenzidine (DAB; Sigma-Aldrich), chloramphenicol (Sigma-Aldrich), and hydrogen peroxide (Sigma-Aldrich) for 1 min, at room temperature, and washed in water. Finally, the strips were scanned with an Epson Perfection 4990 photo scanner.

Immunostaining Analyses

To evaluate the in situ expression of proteins analyzed by Western blotting, we performed immunostaining using the immunoperoxidase method and immunofluorescence. Slides were analyzed by light, confocal, or two-photon microscopy (to perform three-dimensional analysis of the Leydig cell cytoarchitecture in the collared peccary testis parenchyma). The tissue samples were fixed in Bouin solution and embedded in Paraplast (Sigma-Aldrich). Sections (thickness, 5 μm) were cut and used for the immunoperoxidase reaction and immunofluorescence staining. For two-photon microscopic analysis, sections with a thickness of 300 μm were used.

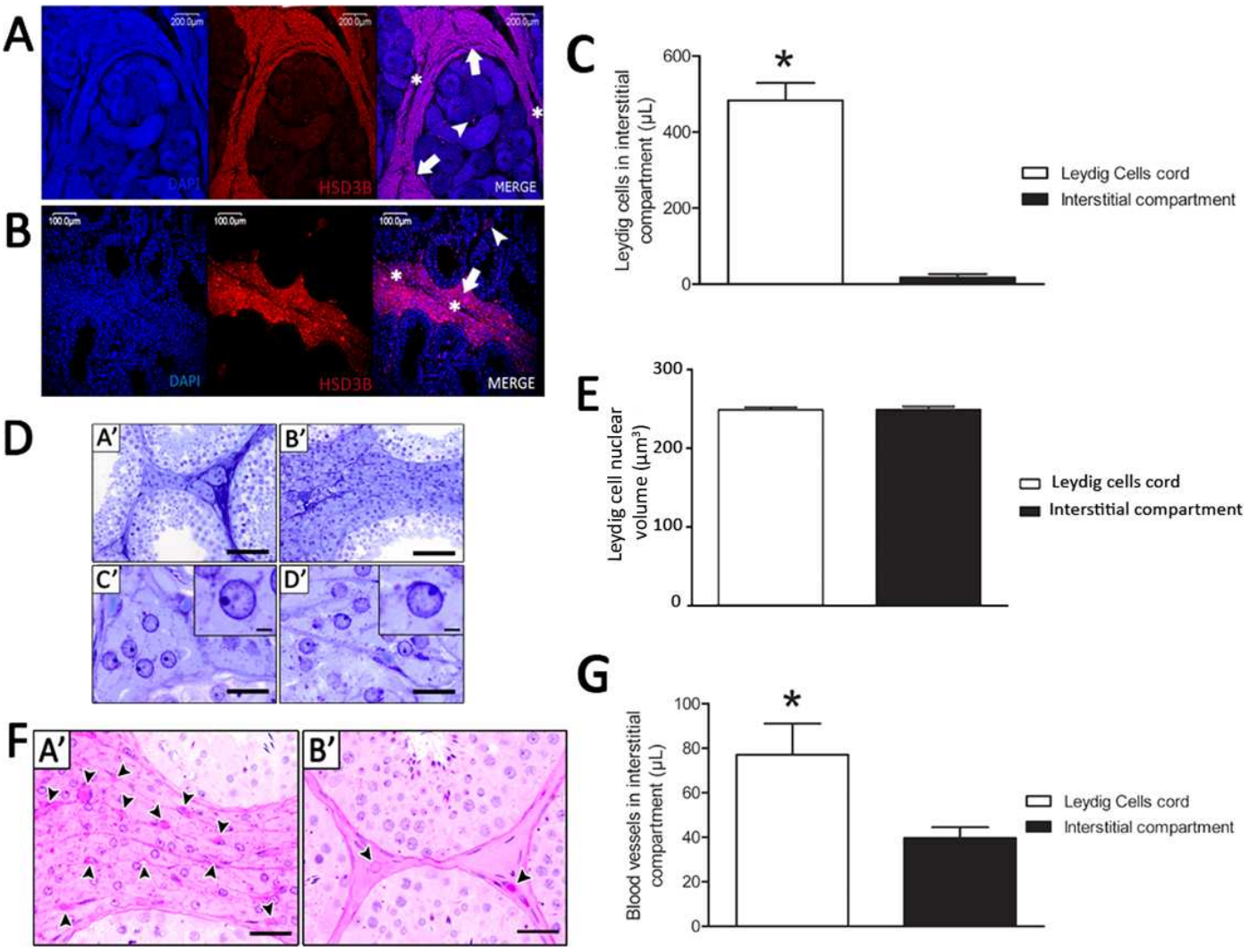

FIG. 1. Leydig cell (LC) cytoarchitecture, nuclear size and blood vessel volume (µl) in the collared peccary testis parenchyma. As expected, HSD3B immunolocalization was observed only in LCs, particularly on those forming cords surrounding the seminiferous tubule (ST) lobes (arrow) and externally delimited by dense connective tissue (asterisk; **A** and **B**). However, few HSD3B- LCs (arrowhead) were also present among the STs (**A**, **B**, and **C**; $*P < 0.05$). No nuclear volume difference ($P > 0.05$) was observed for LCs located in the areas among (**DA′** and **DC′**) or surrounding (**DB′** and **DD′**) the STs (**E**), whereas the blood vessels volume (µl) was significantly higher in the areas where LCs were surrounding the STs (**FA′** and **G**; $*P < 0.05$). See also Supplemental Movie S1. Bar = 200 µm (**A**), 100 µm (**B**), 70 µm (**DA′** and **DB′**), 35 µm (**DC′** and **DD′**), 3 µm (**D**, **insets**), and 50 µm (**FA′** and **FB′**).

Tissue sections were immunostained using protocols specifically developed for each antigen and with antibody dilutions previously tested. After dewaxing and rehydration, antigen retrieval was performed in citrate buffer (pH 6.0) for 5 min after boiling in a microwave oven for approximately 10 min. For immunohistochemistry, endogenous peroxidase was quenched for 30 min with 3% H_2O_2 (Sigma-Aldrich) in PBS. Nonspecific binding was blocked with Ultra-V-Block (Thermo Scientific). Primary antibodies for GFRA1 (SC-6157, 1:500; Santa Cruz Biotechnology) were applied, and the slides were incubated at 4°C overnight. Biotinylated anti-goat IgG antibodies (1:100) were applied and incubated for 60 min at room temperature. Detection of the signal was performed by incubating the section in streptavidin for 10 min, followed by reaction with peroxidase substrate diaminobenzidine and counterstaining with hematoxylin (Merck) at room temperature. Following dehydration, sections were mounted and analyzed.

To quantify the percentage of A_{und} spermatogonia (characterized according to morphological criteria) that were $GFRA1^+$, 200 A_{und} cells were randomly evaluated for each peccary (n = 5).

For immunofluorescence, nonspecific background was blocked for 5 min with Ultra-V-Block incubation at room temperature. Tissue sections were then incubated overnight at 4°C with primary antibodies at the following dilutions: GFRA1, 1:25; CSF1, 1:200; CSF1R, 1:100; 3β-hydroxysteroid dehydrogenase (HSD3B; SC-30820; Santa Cruz Biotechnology), 1:500; or VASA (DDX4, specific germ cell marker; Ab13840; Abcam), 1:200. Antigens were detected by incubation with Alexa Fluor secondary antibodies (488 anti-rabbit [1:500] and/or 546 anti-goat [1:300]) for 1 h at room temperature. After nuclear counterstaining using 4′,6-diamidino-2-phenylindole (Sigma-Aldrich), sections were mounted with Mowiol 4–88 solution (Merck).

Confocal and Two-Photon Laser-Scanning Microscopy and Image Acquisition

Confocal images were obtained using a 40× oil-immersion objective and a 510 META Laser Scanning Confocal Microscope (Zeiss) equipped with 488-, 543-, and 633-nm lasers. Dual- and triple-channel images were obtained by sequential scanning. Two-photon microscopy was performed with a system mounted onto the laser-scanning confocal microscope (FV300; Olympus). The multiphoton laser was a Coherent Chameleon Ultra High Power Ti:Sapphire Laser (pulse, 140 fsec; Coherent) with a wavelength of 680-1080 nm.

For image analysis, we used the ImageJ software (National Institutes of Health; http://rsb.info.nih.gov/ij/). Laser power and acquisition settings were adjusted to produce submaximal pixel values in the testis tissue sections. Background subtraction and contrast/brightness enhancement (up to 20% enhancement using the maximum slider in ImageJ) were performed identically for all the images in the same experiment.

Statistical Analyses

All data were tested for normality and homoscedasticity of the variances. Parametric data were analyzed by ANOVA and differences compared by Tukey test, whereas Student *t*-test was used for two-parameter analysis. Nonparametric data were compared by chi-square test. All analyzes were performed using the GraphPad Prism (Version 5; GraphPad Software, Inc.) and SAEG software (Federal University of Viçosa, Brazil). and SAEG software. All data were expressed as the mean ± SD, and the level for significance was $P < 0.05$.

RESULTS

Leydig Cell Distribution in the Testis Parenchyma

Immunostaining analysis in three-dimensional reconstruction of the testis parenchyma using HSD3B, an enzyme specific to steroidogenic cells, confirmed recent results from our laboratory showing that in collared peccaries, Leydig cells present a unique cytoarchitecture [19]. Hence, Leydig cells forming structures like cords (externally delimited by dense connective tissue) surrounding the seminiferous tubule lobes were readily observed, whereas few HSD3B-positive Leydig cells, probably representing projections from the cords (see Supplemental Movie S1; all Supplemental Data are available online at www.biolreprod.org), were detected between the seminiferous tubules (Fig. 1, A and B). In this regard, the volume occupied by the Leydig cells in the cord-like structures in comparison to those present in the intertubular space was almost 30-fold higher ($P < 0.05$) (Fig. 1C). However, no differences were found in nuclear volumes of Leydig cells present in the cords or between the tubules ($P > 0.05$) (Fig. 1, D and E). We also observed a higher vascular network in the Leydig cell cord space in comparison to the space between seminiferous tubules ($P < 0.05$) (Fig. 1, F and G).

Stages of the Seminiferous Epithelial Cycle

Based on the development of the acrosomal system in spermatids, 10 stages of the seminiferous epithelial cycle were characterized in collared peccaries (Fig. 2). The spermiogenic phase was divided in 16 steps, and the mature spermatids were released (spermiated) in the tubular lumen at stage VI, which presented the higher frequency (~21%) (bottom of Fig. 2), followed by stages VII–IX, which showed similar frequencies (~14%). The frequencies presented by the remaining stages were from approximately 5% to 8%.

Spermatogonial Morphology, Size, and Kinetics

Based on the criteria used [22], spermatogonial cells in collared peccaries were characterized as type A (A_{und}, A_1, A_2, A_3, and A_4), In, and type B spermatogonia (Fig. 3A). Because of the absence of clear morphological criteria, A_{und} spermatogonia encompassed A_s, A_{pr}, and A_{al} spermatogonia. Almost all of these cells (92.7% ± 1.2%) were $GFRA1^+$ (Fig. 3, B and E).

Morphologically, the A_{und} spermatogonium showed a mottled or granular spherical nucleus with little heterochromatin and a single prominent and rounded nucleolus. Four generations of differentiating type A spermatogonia were characterized (A_1, A_2, A_3, and A_4), and overall, these cells presented a light and finely granular euchromatin. Heterochromatin was not observed in type A_1 spermatogonia, whereas the amount of heterochromatin gradually increased from type A_2 to type A_4 spermatogonia. Both In and type B spermatogonia showed ovoid nuclei and presented an increased euchromatin and heterochromatin granularity, which gave the nucleoplasm a very granular aspect. In contrast to the A_{und} spermatogonia, which were present in all stages of the seminiferous epithelium cell cycle, differentiating spermatogonia were observed in well-defined stages of cycle (Fig. 2). Therefore, types A_1, A_2, A_3, and A_4 spermatogonia were found in stages VIII, IX, X, and I, respectively. The In spermatogonia were observed in stages II–IV, and type B spermatogonia were present in stages V–VII.

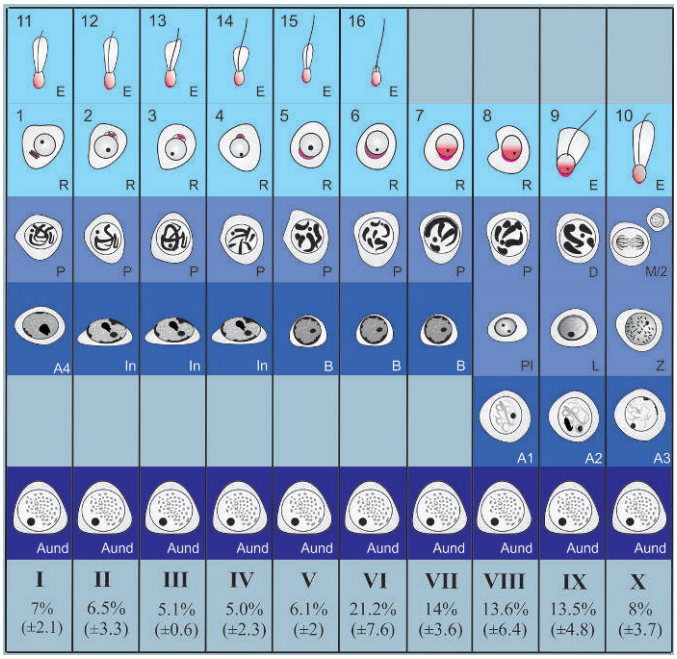

FIG. 2. Diagram illustrating the 10 stages of the seminiferous epithelial cycle (SEC) characterized in the collared peccary based on the acrosomic system. The relative stage frequencies are also shown at the bottom (mean ± SD). Roman numerals indicate the 10 different stages of the SEC. The following germ cell types are depicted: A_{und} spermatogonia (A_s, A_{pr}, and A_{al}), differentiated type A (A_1, A_2, A_3, and A_4), In, and type B spermatogonia. Arabic numerals (1–16) indicate each step of the spermatid acrosome (red) development in the collared peccary. D, diplotene; L, leptotene; M/2, meiotic figure and secondary spermatocyte; P, pachytene; Pl, preleptotene; Z, zygotene.

Stereological analysis indicated that A_{und} spermatogonia exhibited a significantly higher nuclear volume in comparison to the other spermatogonia ($P < 0.05$) (Fig. 3C). No significant differences were observed among differentiating type A spermatogonia, whereas type B spermatogonia presented the smallest nuclear volume ($P < 0.05$). Spermatogonial cell kinetics indicated gradually increasing cell numbers from type A_1 to type B spermatogonia, whereas in comparison to the other stages, the A_{und} spermatogonia showed higher numbers ($P < 0.05$) at stages VI and VII (Fig. 3D), just before differentiation to type A_1 spermatogonia.

Spermatogonial Distribution

According to the three seminiferous tubule regions characterized (Fig. 4A) and based on the morphological criteria used, the A_{und} spermatogonia were mainly located ($P < 0.05$) in the T-I region adjacent to the intertubular compartment without Leydig cells ($P < 0.05$) (Fig. 4B). In contrast, this cell type was less frequently seen in the region in contact with Leydig cells (T-LC; $P < 0.05$) (Fig. 4B). The type A_1 spermatogonia presented a preferential location for the T-I and T-T regions ($P < 0.05$) (Fig. 4B). However, the other spermatogonial cell types (A_2, A_3, A_4, In, and B) were evenly distributed along the seminiferous tubule cross-sections ($P > 0.05$) (Fig. 4B). Regarding the analysis of the spermatogonial cell type distribution in the inner seminiferous tubules that do not face to the LC cords (T-T and T-I), it was observed that

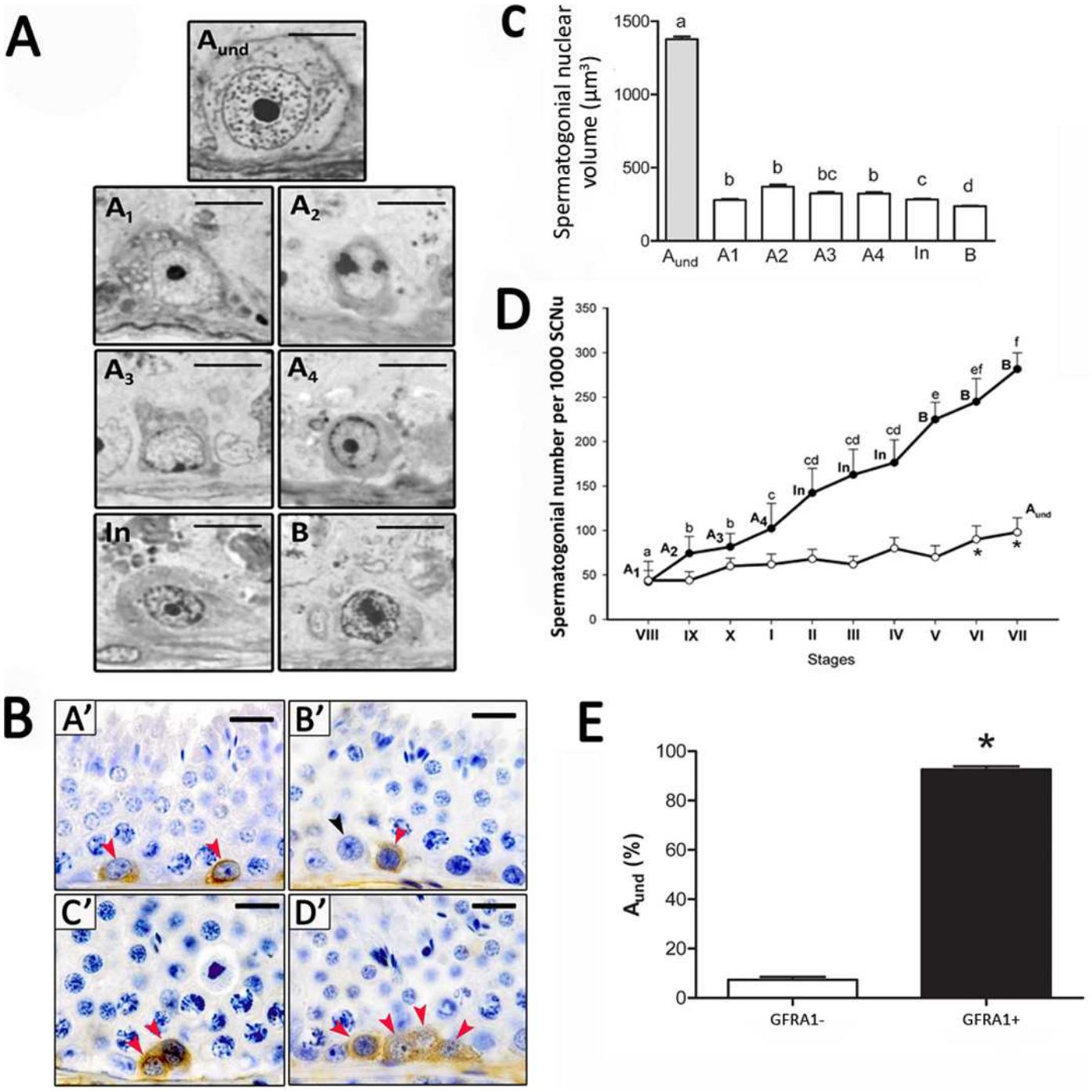

FIG. 3. Morphological, stereological, and molecular characterization of different spermatogonial types in the collared peccary. **A**) High-resolution light photomicrographs of the collared peccary's spermatogonial subtypes (A_{und}, A_1, A_2, A_3, A_4, In, and B spermatogonia) showing nuclear details that allows their identification. **B**) Immunostaining positive for GFRA1 was found in A_{und} spermatogonia in collared peccaries (red arrowheads in **A′**, **B′**, **C′**, and **D′**). However, GFRA1-negative A_{und} spermatogonia were also observed (black arrowhead in **B′**). Nuclear morphology and size of these GFRA1$^+$ cells were very similar to those observed for A_{und} spermatogonia. **C**) The nuclear volume of the different spermatogonial types was evaluated, showing that A_{und} spermatogonia (encompassing A_s, A_{pr}, and A_{al} spermatogonia) presented the highest (different superscript letters denote significant differences, $P < 0.05$) nuclear volume, whereas type B spermatogonia presented the lowest volume. **D**) Number of A_{und} (white circles) and differentiated (black circles) spermatogonial subtypes per 1000 Sertoli cell nuclei (SCNu) observed along the 10 stages of the SEC in collared peccaries, indicating their proliferation rate (kinetics; different superscript letters denote significant differences, $P > 0.05$). **E**) Percentage of GFRA1$^+$ spermatogonia in the A_{und} population. Asterisk (*) in **D** and **E** denotes significant difference ($P < 0.05$). Bar = 5 µm (**A**) and 40 µm (**B**).

A_{und} spermatogonia also had a preferential location for the T-I region ($P < 0.05$) (Fig. 4C), whereas the other spermatogonial types (A_1 to B) were evenly distributed in the T-T and T-I regions (Fig. 4C). Particularly in the T-I region, we observed that the A_{und} spermatogonia had a preferential location for the areas with blood vessels, whereas differentiating spermatogonial types (A_1 to B) and Sertoli cells were randomly distributed in relation to this parameter ($P < 0.05$) (Fig. 4, D and E).

As shown in Figure 5, when all the three regions were subdivided into peripheral (50% of total) and central (50% of

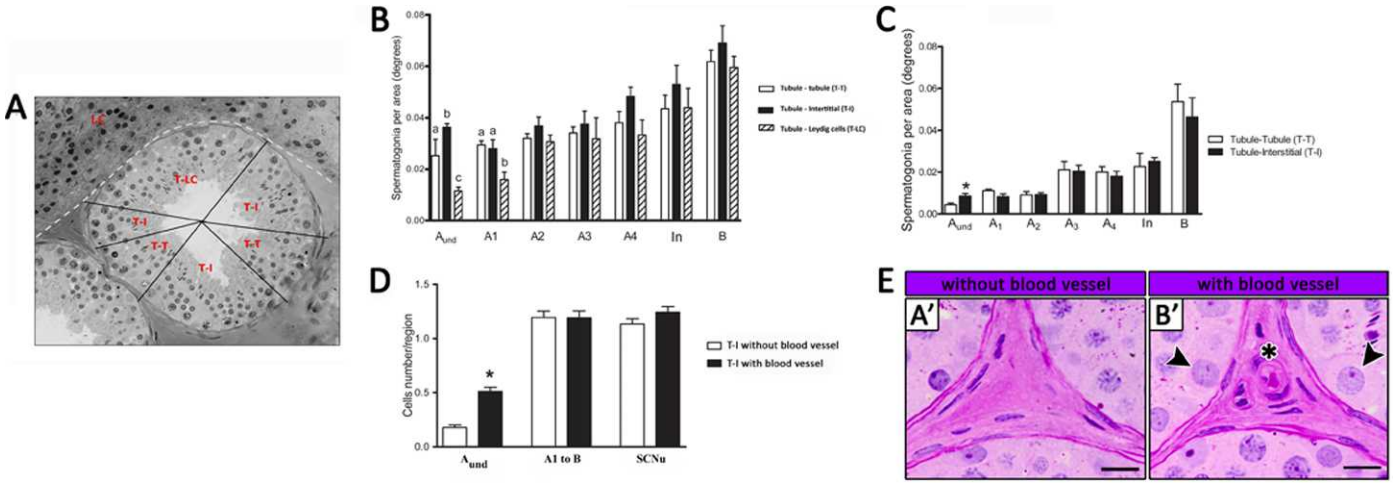

FIG. 4. **A**) Spermatogonial distribution along the seminiferous tubule perimeter based on three previously established regions: T-T, T-I, and T-LC. **B**) A_{und} spermatogonial cells were preferentially located (different superscript letters denote significant differences, $P < 0.05$) in the T-I region, and the type A_1 spermatogonia presented a preferential location for the T-I and T-T regions. The remaining spermatogonial types were randomly distributed along the seminiferous tubule perimeter. **C**) In the inner seminiferous tubules that do not face the LC cords (T-T and T-I), A_{und} spermatogonia had a preferential location ($^*P < 0.05$) for the T-I region, whereas the other spermatogonial types (A_1 to B) were evenly distributed in the T-T and T-I regions. **D**) Considering only the T-I region, A_{und} spermatogonia were preferentially ($^*P < 0.05$) located in areas with blood vessels, an aspect that was not observed for differentiated spermatogonial types (A_1 to B) and Sertoli cell nuclei (SCNu). **E**) Representative pictures illustrating that the A_{und} spermatogonia (arrowheads; **B′**) have "preferential" location for T-I areas with blood vessels (asterisk; **B′**). Bar = 20 μm.

total) areas, in T-T and T-I, A_{und} spermatogonia were preferentially located ($P < 0.05$) in the peripheral and central area, respectively (Fig. 5, A–D), an aspect observed for the type A_1 spermatogonia ($P < 0.05$) in T-LC central area (Fig. 5, E and F). In this kind of analysis, no preferential location ($P > 0.05$) was observed for type A_2 to type B spermatogonia.

GFRA1 and CSF1R Immunostaining and Western Blot Analysis

Immunostaining for GFRA1 was observed for A_{und} spermatogonia encompassing cell types considered to be A_s, A_{pr}, and A_{al} spermatogonia (Fig. 6, A–C). The evaluation of GFRA1$^+$ spermatogonial cell distribution in the three different regions considered in the present study demonstrated a preferential location ($P < 0.05$) of these cells for the region adjacent to the interstitial compartment without Leydig cells (T-I) (Fig. 6F). The presence of GFRA1 protein (~47 kDa) was confirmed by immunoblotting assay (Fig. 6E).

As shown in Figure 7, CSF1R expression was found in spermatogonia (Fig. 7, A and D) as well as in Leydig cells (Fig. 7, A, C, and D). However, its ligand, CSF1, was observed in both Leydig and peritubular myoid cells (Fig. 7, E and F). Double staining for GFRA1 and CSF1R demonstrated that all GFRA1$^+$ cells were also CSF1R$^+$ (Fig. 7, A–D). Expression of CSF1 (~30 kDa) and its receptor, CSF1R (~130 kDa), was

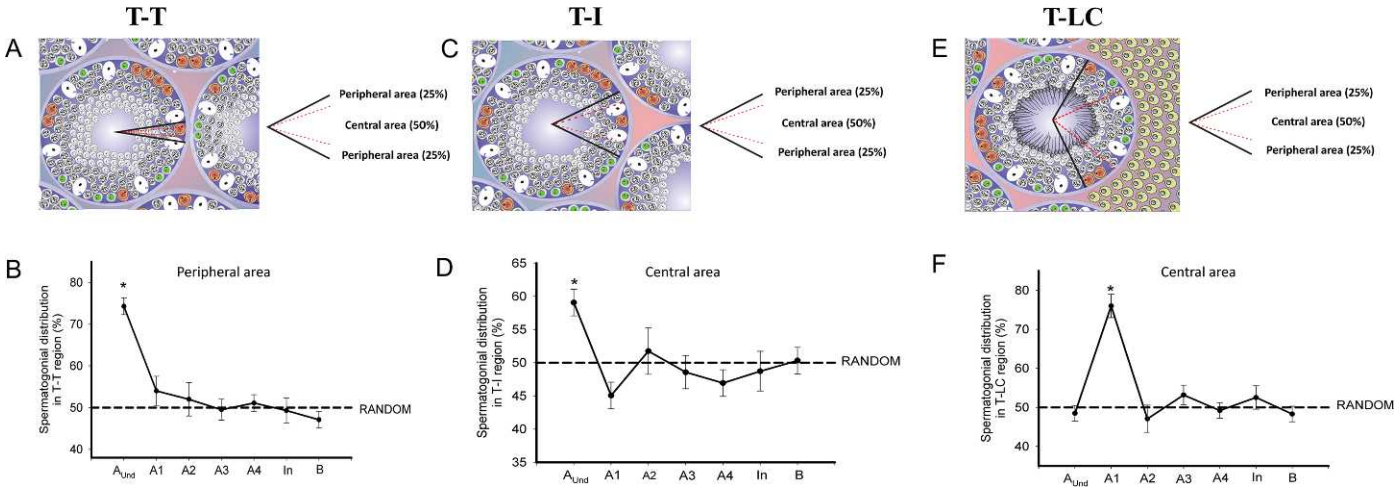

FIG. 5. Spermatogonial distribution in the three established regions mentioned in Figure 4. **A**, **C**, and **E**) T-T (**A**), T-I (**C**), and T-LC (**E**) contact. To have a more precise evaluation, these regions were subdivided into peripheral (delimited externally by black lines) and central (delimited by dotted red lines) areas. **B**, **D**, and **F**) Spermatogonial cell frequency distributions in relation to the peripheral (T-T) and central (T-I and T-LC) areas. As observed in the T-T region, few A_{und} spermatogonial cells ($^*P < 0.05$) were observed in the central area (**B**). Although much more A_{und} were found in the T-I region, these cells were more concentrated ($^*P < 0.05$) in the central area (**D**). Regarding the T-LC region, the differentiated type A_1 spermatogonia presented a preferential location ($^*P < 0.05$) in the central area, whereas all the other spermatogonial types (A_{und}, A_2, A_3, A_4, In, and B) were randomly ($P < 0.05$) distributed in this region (**F**). Except for type A_1 spermatogonia in the T-LC region, all differentiated spermatogonia presented a random distribution.

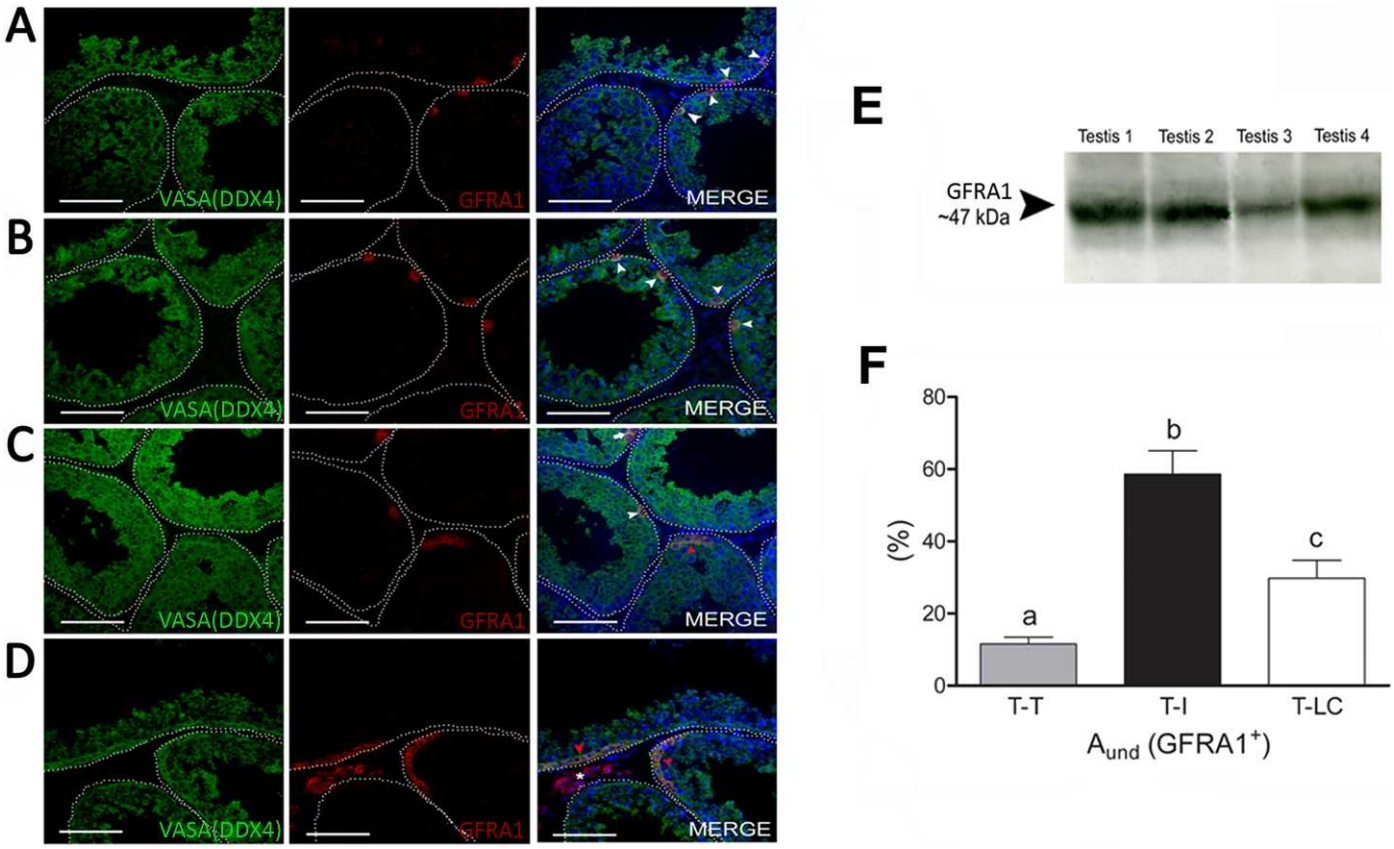

FIG. 6. Undifferentiated spermatogonial immunostaining and distribution along the seminiferous tubule cross-sections. As indicated in all merged figures, GFRA1 expression was observed in A_{und} spermatogonial cells and colocalized with DDX4 (VASA) expression (specific germ cell marker). This expression was found in A_{und} spermatogonia (**A**–**D**; white arrow and white arrowheads indicate small chains of A_{und}, whereas red arrowhead indicates large chains of A_{und}). Immunoblotting in the testis parenchyma representing the whole testis (n = 4) confirmed the expression of GFRA1 in this organ (**E**). $GFRA1^+$ cells were preferentially located in the region in contact with the interstitial compartment (**F**), strongly suggesting that the SSC niche is located in this region. Different superscript letters denote significant differences ($P < 0.05$). The asterisk in the merged image in **D** represents a small cluster of Leydig cells. Bar = 50 μm (**A**–**D**).

also detected in the collared peccary testis lysates (Fig. 7G). The immunohistochemistry and the immunoblotting negative controls are shown in the Supplemental Figure S1.

DISCUSSION

Previous studies in our laboratory showed that collared peccaries present a peculiar Leydig cell organization in which these steroidogenic cells surround the seminiferous tubule lobes [19]. In the present study, we used this species as a unique model to assess the role of Leydig cells in SSC physiology. To this effect, we investigated in more detail Leydig cell cytoarchitecture and characterized the seminiferous epithelial cycle according to the acrosomal system. These approaches allowed us to morphologically describe the different types of spermatogonia in the peccary and their location in three different regions of the seminiferous tubules. Based on the distribution of $GFRA1^+$ spermatogonia in relation to Leydig cells, our results strongly suggest that instead of being critical for SSC self-renewal and maintenance, Leydig cells might play an important role in the spermatogonial commitment to differentiation. In addition, the pattern of expression of CSF1/CSF1R suggests that peritubular myoid cells may play a substantial role in SSC physiology.

In the only report, to our knowledge, related to Leydig cell distribution and arrangement in mammals ([20] and reviewed in Russell [21]), three different patterns were characterized. Briefly, in pattern I, observed in several rodent species, Leydig cells and the connective tissue occupy a relatively small percentage of the interstitium. In pattern II, described in ruminants and primates (including humans), Leydig cells are scattered in abundant connective tissue. Finally, in pattern III, as found in domestic pigs and zebra, abundant groups of Leydig cells occupy almost all the interstitium. In peccaries, the Leydig cell volume density is similar to that in pigs [19]. However, collared peccaries present a different and unique Leydig cell arrangement, because these cells surround the seminiferous tubule lobes and are rarely seen within the intertubular compartment [19]. In the present study, z-stack reconstruction of the testis parenchyma allowed us to confirm this peculiar arrangement. Moreover, we observed many more blood vessels in the Leydig cell cords than in the intertubular areas without Leydig cells. These results underscore the possibility of a cross-talk between Leydig cells and the vascular network and suggest a role of Leydig cells in controlling testicular angiogenesis and blood flow [25]. A reciprocal situation could also be true—namely, that blood factors control Leydig cell numbers and architecture [25]. Based on the similarities observed for nucleus size and overall cell morphology, Leydig cells located between the seminiferous tubules are an extension from the cells observed in the cords. This aspect was demonstrated in the present study using z-stack reconstruction.

In comparison to the other types, A_{und} spermatogonia showed a prominent nuclear volume. This particularity, not investigated

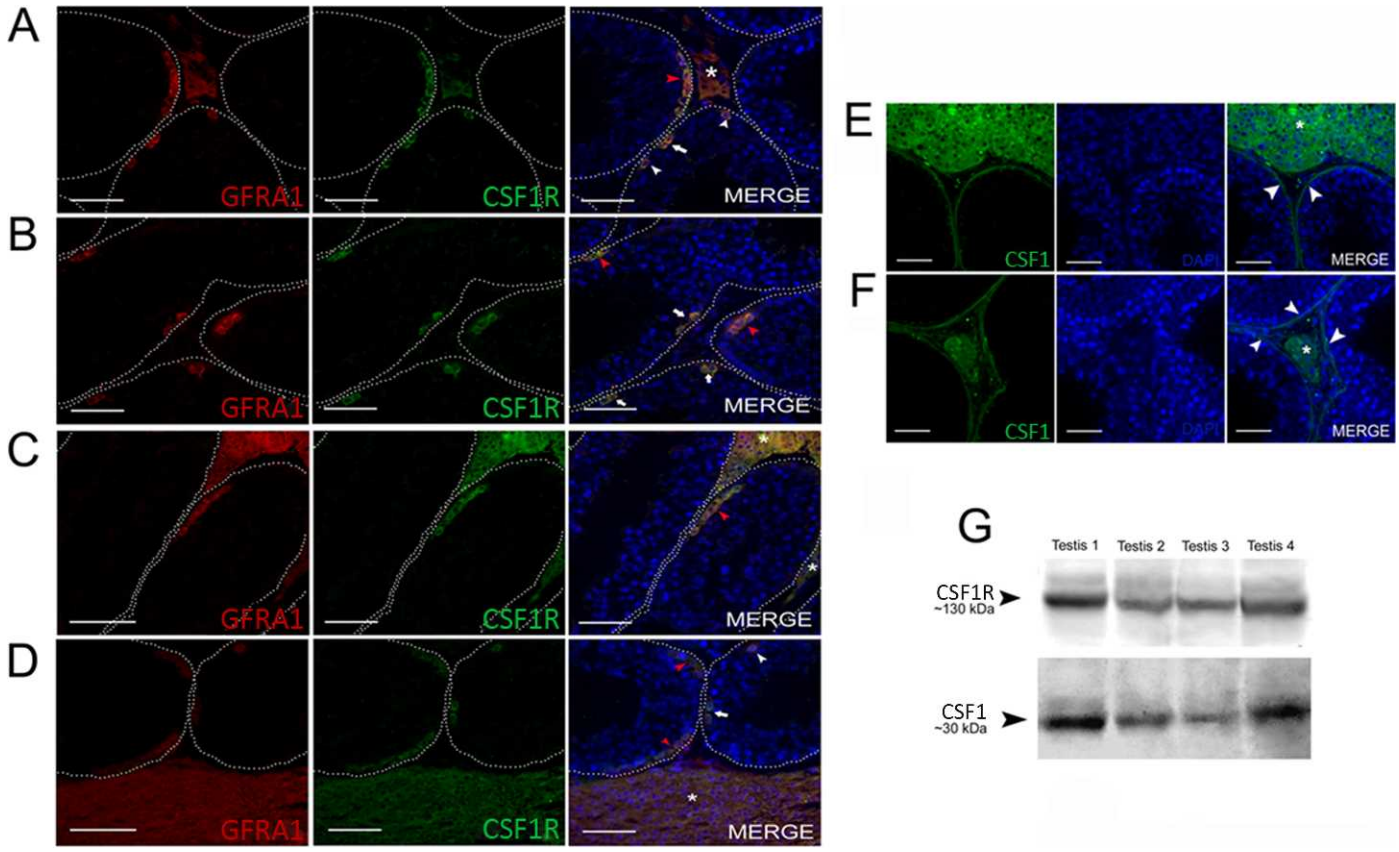

FIG. 7. CSF1/CSF1R expression in collared peccary spermatogonia. Expression of CSF1R colocalized with GFRA1$^+$ cells, including A_s (**A** and **D**; white arrowhead), A_{pr} (**A**, **B**, and **D**; white arrow), and A_{al} (**A**, **C**, and **D**; red arrowhead) spermatogonia. As illustrated in **A**, **C**, and **D** (asterisk), Leydig cells also presented colocalized immunostaining for CSF1R and the GFRA1 receptors. Regarding CSF1, ligand to CSF1R, labeling was observed in Leydig cells (**E** and **F**; asterisk) and peritubular myoid cells (**E** and **F**; arrowhead). **G**) Western blot analysis demonstrated that CSF1 and CSF1R are expressed in whole-testis tissue samples (n = 4). Bar = 50 μm.

in other suiform species, allowed us to accurately identify A_{und} spermatogonia in the basal compartment of the seminiferous epithelium.

The morphology of germ cells in peccaries is similar to that described for domestic and wild pigs [26–28]. However, considering that in peccaries, type B spermatogonia only form preleptotene spermatocytes after spermiation, the overall germ cell associations in this species rather resemble those observed in wild boars [28], whereas the stage frequencies grouped in the premeiotic and postmeiotic phases of spermatogenesis, which are considered to be phylogenetically related, are very similar in these three suiform species [19, 28]. In relation to the spermatogonial phase of spermatogenesis, at least seven spermatogonial types were characterized in collared peccaries (A_{und}, A_1, A_2, A_3, A_4, In, and B), and this number (not discriminating A_s, A_{pr}, and A_{al} spermatogonia) is quite similar to that found in domestic pigs [26, 27]. This indicates that the number of spermatogonial generations is also phylogenetically determined [1, 27].

According to data compiled from other species [1, 11], including pigs [27], kinetics of differentiating spermatogonia show a gradual increase in cell numbers from type A_1 to type B spermatogonia. In peccaries, a significant germ cell loss occurs, particularly from type A_2 to type A_4 spermatogonia [1, 11, 27], in which cell density in the seminiferous epithelium is known to be regulated [1, 29]. The kinetics of A_{und} spermatogonia in peccaries follow a trend similar to that found in domestic pigs [26] and in rodents [1, 30–32], where a higher number of A_{und} spermatogonia is observed at the stages close to spermiation—namely, just before type A_{al} differentiation to type A_1 spermatogonia [1, 30–32].

Regarding the physiology of SSCs within their niche, our findings demonstrated that A_{und} spermatogonia were mainly located in regions adjacent to blood vessels, confirming that the vascular network may play an important role in the regulation of SSCs [15]. On the other hand, in the peccary, Leydig cells seem to play a role in spermatogonial differentiation (i.e., in the A_{al}-to-A_1 transition). In this respect, the gradual niche deviation observed in the present study corroborates the hypothesis that SSCs lose their contact with the niche when they are committed to differentiation [33, 34].

To our knowledge, the present study is the first to investigate the distribution of GFRA1$^+$ spermatogonia in mammalian seminiferous tubule cross-sections, taking into consideration the whole-testis parenchyma. In peccaries, A_{und} spermatogonia (encompassing A_s to A_{al} spermatogonia) expressed GFRA1, and these cells were preferentially located in the region close to the interstitial compartment without Leydig cells (T-I). This is an important finding that may apply to other mammalian species or even to other vertebrate groups [35]. In addition, according to the morphological data obtained in the present study, we found that type A_1 spermatogonia have a preferential location for the T-LC central area (Fig. 5). This finding further supports the hypothesis that Leydig cell products might mediate spermatogonial differentiation. Further studies are needed to investigate the factors or mechanisms controlling the commitment of A_{und} spermatogonia to differentiation, which would take into consideration the complexity of A_{und} homeostasis [5, 34–36]

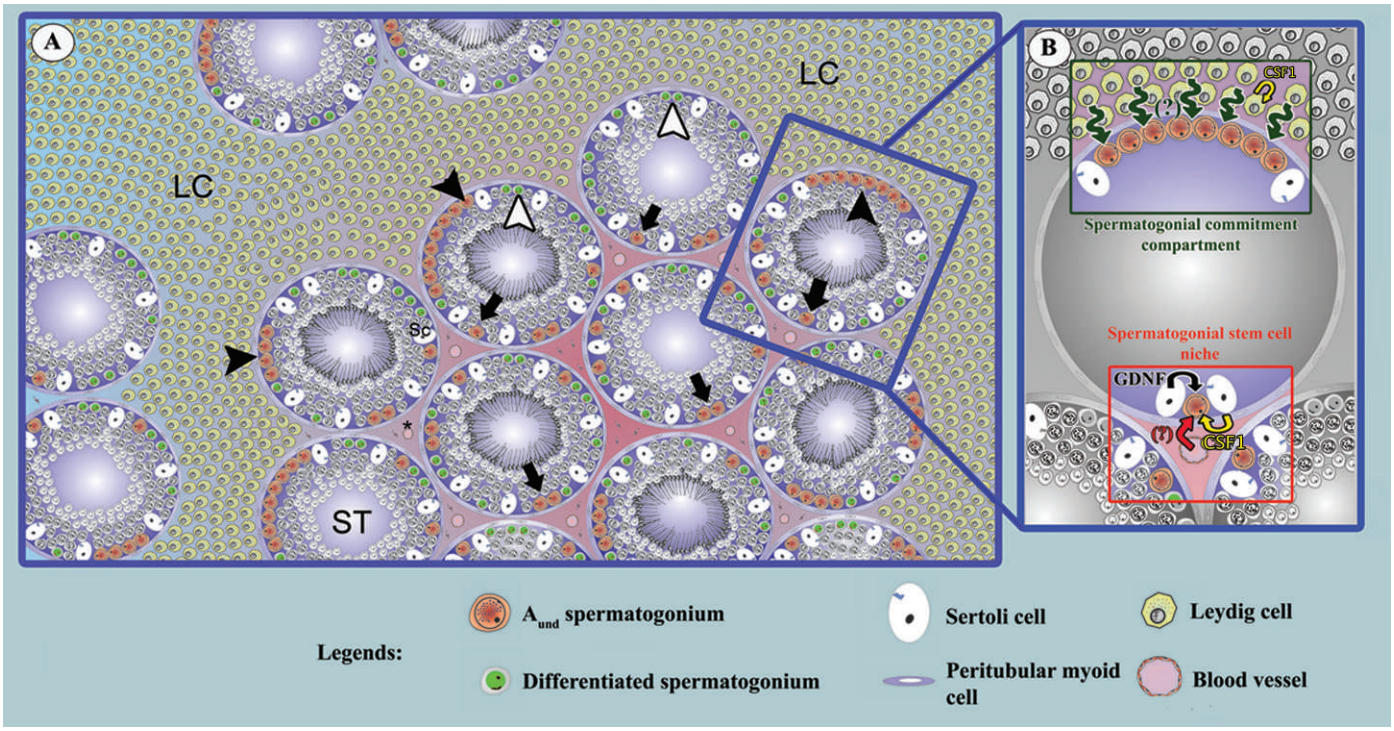

FIG. 8. **A** and **B**) Major results obtained for the collared peccary, in which a unique Leydig cell cytoarchitecture was observed in the testis parenchyma. Taking advantage of this particular cytoarchitecture, we observed that the A_{und} spermatogonia (arrow) showed preferential location for the region in contact with the interstitial compartment without Leydig cells, strongly suggesting that the SSC niche and/or spermatogonial self-renewal in this species is not dependent, at least not directly, on Leydig cells but, instead, is regulated by factors from the interstitium without steroidogenic elements and the vasculature. As depicted in this figure, peritubular myoid cells may also play an important role in the SSC niche through their production of CSF1. LC, Leydig cells forming cords; SC, Sertoli cell; ST, seminiferous tubules. Black arrowheads indicate large chains of A_{und} spermatogonia while white arrowheads show differentiated spermatogonia.

as well as the relationships between germ cells and somatic cells during the different stages of spermatogenesis.

The A_{al}-to-A_1 transition usually occurs around spermiation at stages considered to be androgen-dependent [24, 37]. Perhaps not by coincidence, Sertoli cells produce less GDNF at these stages [38]. Therefore, the relationship between the SSC niche and androgens has been recently investigated [7, 13], but the mechanisms by which testosterone regulates somatic and germ cell function in the testis remain unclear [13, 39]. Particularly, it is already established that in mammals, androgen receptor expression in germ cells is not required for spermatogenesis [40], whereas the inhibition of testosterone promotes spermatogonial self-renewal and better colonization after SSC transplantation in mice [41, 42]. Also, higher key steroidogenic gene expression and higher testosterone level in recipient zebrafish testes result in a prodifferentiation microenvironment, with subsequent SSC commitment to differentiation [35]. Taken together, these results again strongly suggest a role for Leydig cells in spermatogonial differentiation.

Because Leydig cells express CSF1 in mice [17, 18], a role for Leydig cells in SSC self-renewal via CSF1/CSF1R signaling was recently suggested [17, 18]. The present study shows production of CSF1 by Leydig cells in peccaries as well. In addition, we found CSF1R expression in all $GFRA1^+$ cells. However, because CSF1 is also produced by peritubular myoid cells, and because Leydig cells are rarely seen in the intertubular compartment, we deduce that at least in the peccary, peritubular myoid cells, and not Leydig cells, play a major role in the regulation of SSC self-renewal.

The major results of the present study are illustrated in Figure 8. In summary, taking advantage of the unique Leydig cell cytoarchitecture in collared peccaries and using morphological and immunolabeling approaches for GFRA1 and CSF1/CSF1R, we observed that A_{und} spermatogonia were preferentially located in the region adjacent to the interstitial compartment without Leydig cells. This feature strongly suggests that the SSC niche in this species might not be dependent, at least not directly, on Leydig cells but, rather, on factors derived from peritubular myoid cells, interstitial cells, and the vasculature. Also, as depicted in Figure 8, peritubular myoid cells probably play an important role in the CSF1-dependent self-renewing response of SSCs.

ACKNOWLEDGMENT

The microscopic data in the present study were obtained using the Zeiss 510 Meta confocal microscope from the Center of Electron Microscopy (CEMEL- ICB/UFMG) and from the Biophotonics Laboratory, Department of Physics (UFMG). Technical help from Mara Lívia Santos is highly appreciated. The scholarships awarded to P.H.A.C.-J., G.M.J.C., and S.M.S.N.L. from the FAPEMIG and CNPq are fully appreciated.

REFERENCES

1. de Rooij DG, Russell LD. All you wanted to know about spermatogonia but were afraid to ask. J Androl 2000; 21:776–798.
2. Huckins C. The spermatogonial stem cell population in adult rats. 3. Evidence for a long-cycling population.Cell Tissue Kinet 1971; 4: 335–349.
3. Oakberg EF. Spermatogonial stem-cell renewal in the mouse. Anat Rec 1971; 169:515–531.
4. Huckins C, Oakberg EF. Morphological and quantitative analysis of spermatogonia in mouse testes using whole mounted seminiferous tubules. Anat Rec 1978; 192:519–528.
5. Nakagawa T, Sharma M, Nabeshima Y, Braun RE, Yoshida S. Functional

hierarchy and reversibility within the murine spermatogenic stem cell compartment. Science 2010; 328(5974):62–67.
6. Simon L, Ekman GC, Kostereva N, Zhang Z, Hess RA, Hofmann MC, Cooke PS. Direct transdifferentiation of stem/progenitor spermatogonia into reproductive and nonreproductive tissues of all germ layers. Stem Cells 2009; 27:1666–1675.
7. Caires K, Broady J, Mclean D. Maintaining the male germline: regulation of spermatogonial stem cells. J Endocrinol 2010; 205:133–145.
8. Chiarini-Garcia H, Hornick JR, Griswold MD, Russell LD. Distribution of type A spermatogonia in the mouse is not random. Biol Reprod 2001; 65: 1179–1185.
9. Chiarini-Garcia H, Raymer AM, Russell LD. Nonrandom distribution of spermatogonia in rats: evidence of niches in the seminiferous tubules. Reproduction 2003; 126:669–680.
10. do Nascimento HF, Drumond AL, França LR, Chiarini-Garcia H. Spermatogonial morphology, kinetics and niches in hamsters exposed to short- and long-photoperiod. Int J Androl 2009; 32:486–497.
11. Chiarini-Garcia H, Alves-Freitas D, Barbosa IS, Almeida FR. Evaluation of the seminiferous epithelial cycle, spermatogonial kinetics and niche in donkeys (*Equus asinus*). Anim Reprod Sci 2009; 116:139–154.
12. Hofmann MC. Gdnf signaling pathways within the mammalian spermatogonial stem cell niche. Mol Cell Endocrinol 2008; 288:95–103.
13. Phillips BT, Gassei K, Orwig KE. Spermatogonial stem cell regulation and spermatogenesis. Philos Trans R Soc Lond B Biol Sci 2010; 365: 1663–1678.
14. de Rooij DG. The spermatogonial stem cell niche. Microsc Res Tech 2009; 72:580–585.
15. Yoshida S, Sukeno M, Nabeshima Y. A vasculature-associated niche for undifferentiated spermatogonia in the mouse testis. Science 2007; 317: 1722–1726.
16. Hofmann MC, Braydich-Stolle L, Dym M. Isolation of male germ-line stem cells; influence of GDNF. Dev Biol 2005; 279:114–124.
17. Kokkinaki M, Lee TL, He Z, Jiang J, Golestaneh N, Hofmann MC, Chan WY, Dym M. The molecular signature of spermatogonial stem/progenitor cells in the 6-day-old mouse testis. Biol Reprod 2009; 80:707–717.
18. Oatley JM, Oatley MJ, Avarbock MR, Tobias JW, Brinster RL. Colony stimulating factor 1 is an extrinsic stimulator of mouse spermatogonial stem cell self-renewal. Development 2009; 136:1191–1199.
19. Costa GMJ, Leal MC, Silva JV, Ferreira AC, Guimarães DA, França LR. Spermatogenic cycle length and sperm production in a feral pig species (collared peccary, *Tayassu tajacu*) J Androl 2010; 31:221–230.
20. Fawcett DW, Neaves WB, Flores MN. Comparative observations on intertubular lymphatics and the organization of the interstitial tissue of the mammalian testis. Biol Reprod 1973; 9:500–532.
21. Russell LD. Mammalian Leydig cell structure In: Payne AH, Hardy MP, Russell LD (eds.), The Leydig Cell. Vienna: Cache River Press; 1996:43–96.
22. Chiarini-Garcia H, Russell LD. High-resolution light microscopic characterization of mouse spermatogonia. Biol Reprod 2001; 65: 1170–1178.
23. Russell LD, Ettlin RA, Sinha-Hikim AP. Histological and Histopathological Evaluation of the Testis. Vienna, IL: Cache River Press; 1990.
24. Hess RA, França LR. Spermatogenesis. Cycle of the seminiferous epithelium. In: Cheng CY (ed.), Molecular Mechanisms in Spermatogenesis. Austin, Texas: Landes Bioscience; 2007:1–15.
25. Welsh M, Sharpe RM, Moffat L, Atanassova N, Saunders PT, Kilter S, Bergh A, Smith LB. Androgen action via testicular arteriole smooth muscle cells is important for Leydig cell function, vasomotion and testicular fluid dynamics. PLoS One 2010; 5:e13632.
26. Frankenhuis MT, Kramer MF, de Rooij DG. Spermatogenesis in the boar. Vet Q 1982; 4(2):57–61.
27. França LR, Avelar GF, Almeida FF. Spermatogenesis and sperm transit through the epididymis in mammals with emphasis on pigs. Theriogenology 2005; 63:300–318.
28. Almeida FF, Leal MC, França LR. Testis morphometry, duration of spermatogenesis, and spermatogenic efficiency in the wild boar (*Sus scrofa scrofa*). Biol Reprod 2006; 75:792–799.
29. Russell LD, Chiarini-Garcia H, Korsmeyer SJ, Knudson CM. Bax-dependent spermatogonia apoptosis is required for testicular development and spermatogenesis. Biol Reprod 2002; 66:950–958.
30. de Rooij DG. Spermatogonial stem cell renewal in the mouse. I. Normal situation.Cell Tissue Kinet 1973; 6:281–287.
31. Lok D, Weenk D, De Rooij DG. Morphology, proliferation, and differentiation of undifferentiated spermatogonia in the Chinese hamster and the ram. Anat Rec 1982; 203:83–99.
32. Tegelenbosch RA, de Rooij DG. A quantitative study of spermatogonial multiplication and stem cell renewal in the C3H/101 F1 hybrid mouse. Mutat Res 1993; 290:193–200.
33. Spradling A, Drummond-Barbosa D, Kai T. Stem cells finds their niche. Nature 2001; 414:98–104.
34. Sheng XR, Brawley CM, Matunis EL. Dedifferentiating spermatogonia outcompete somatic stem cells for niche occupancy in the *Drosophila* testis. Cell Stem Cell 2009; 5:191–203.
35. Nóbrega RH, Greebe CD, van de Kant H, Bogerd J, de França LR, Schulz RW. Spermatogonial stem cell niche and spermatogonial stem cell transplantation in zebrafish. PLoS One 2010; 5:e12808.
36. Klein AM, Nakagawa T, Ichikawa R, Yoshida S, Simons BD. Mouse germ line stem cells undergo rapid and stochastic turnover. Cell Stem Cell 2010; 7:214–224.
37. Sharpe R. Regulation of spermatogenesis In: Knobil E, Neill J (eds.), The Physiology of Reproduction, 2nd ed. New York: Raven Press; 1994:1363–1434.
38. Johnston DS, Olivas E, Di Candeloro P, Wright WW. Stage-specific changes in GDNF expression by rat Sertoli cells: a possible regulator of the replication and differentiation of stem spermatogonia. Biol Reprod 2011; 85:763–769.
39. Sadate-Ngatchou PI, Pouchnik DJ, Griswold MD. Identification of testosterone-regulated genes in testes of hypogonadal mice using oligonucleotide microarray. Mol Endocrinol 2004; 18:422–433.
40. Johnston DS, Russell LD, Friel PJ, Griswold MD. Murine germ cells do not require functional androgen receptors to complete spermatogenesis following spermatogonial stem cell transplantation. Endocrinology 2001; 142:2405–2408.
41. Ogawa T, Dobrinski I, Avarbock MR, Brinster RL. Leuprolide, a gonadotropin-releasing hormone agonist, enhances colonization after spermatogonial transplantation into mouse testes. Tissue Cell 1998; 30: 583–588.
42. Dobrinski I, Ogawa T, Avarbock MR, Brinster RL. Effect of the GnRH-agonist leuprolide on colonization of recipient testes by donor spermatogonial stem cells after transplantation in mice. Tissue Cell 2001; 33: 200–207.